

Article

# Diffusion Nonlinear Estimation and Distributed UAV Path Optimization for Target Tracking with Intermittent Measurements and Unknown Cross-Correlations

Shen Wang, Yinya Li , Guoqing Qi and Andong Sheng

School of Automation, Nanjing University of Science and Technology, Nanjing 210094, China

\* Correspondence: liyinya@njust.edu.cn

**Abstract:** This paper focuses on distributed state estimation (DSE) and unmanned aerial vehicle (UAV) path optimization for target tracking. First, a diffusion cubature Kalman filter with intermittent measurements based on covariance intersection (DCKFI-CI) is proposed, to address state estimation with the existence of detection failure and unknown cross-correlations in the network. Furthermore, an alternative transformation of DCKFI-CI based on the information form is developed utilizing a pseudo measurement matrix. The performance of the proposed DSE algorithm is analyzed using the consistency and the bounded error covariance of the estimate. Additionally, the condition of the bounded error covariance is derived. In order to further improve the tracking performance, a UAV path optimization algorithm is developed by minimizing the sum of the trace of fused error covariance, based on the distributed optimization method. Finally, simulations were conducted to verify the effectiveness of the proposed algorithm.

**Keywords:** unmanned aerial vehicle; diffusion cubature Kalman filter; covariance intersection; intermittent measurements; distributed path optimization



**Citation:** Wang, S.; Li, Y.; Qi, G.; Sheng, A. Diffusion Nonlinear Estimation and Distributed UAV Path Optimization for Target Tracking with Intermittent Measurements and Unknown Cross-Correlations. *Drones* **2023**, *7*, 473. <https://doi.org/10.3390/drones7070473>

Academic Editor: Eugenio Cesario

Received: 19 June 2023

Revised: 13 July 2023

Accepted: 17 July 2023

Published: 18 July 2023



**Copyright:** © 2023 by the authors. Licensee MDPI, Basel, Switzerland. This article is an open access article distributed under the terms and conditions of the Creative Commons Attribution (CC BY) license (<https://creativecommons.org/licenses/by/4.0/>).

## 1. Introduction

Unmanned aerial vehicles (UAVs), also known as drones, have been widely applied for target tracking, with versatility and advanced capabilities for civilian and military areas, such as surveillance, environmental monitoring, resource exploration, and so on [1]. The utilization of UAVs for target tracking offers numerous advantages over traditional stationary detection platforms. UAVs exhibit flexible mobility and provide an aerial perspective, allowing them to cover large areas and overcome geographical obstacles [2]. A variety of advanced sensors, such as time-of-arrival (TOA) sensors, angle-of-arrival (AOA) sensors, time-difference-of-arrival (TDOA) sensors, and so on, can be loaded on UAVs, according to the requirements of the target tracking task [3]. In practical applications, UAVs typically engage in target tracking tasks within networked formations [4,5]. In a wireless network, the information of a UAV can only be transmitted to its neighboring UAVs, which enhances the reliability and robustness of the system but poses significant challenges for distributed state estimation, to improve the tracking performance. In addition, leveraging the mobile platform characteristics of UAVs to acquire higher-quality measurements would also contribute to improving tracking performance.

Much previous work in literature has been dedicated to developing different distributed state estimation (DSE) algorithms. Two commonly adopted techniques for addressing DSE are consensus-based and diffusion-based strategies. The concept of the consensus Kalman filter (KF) was proposed in [6] to eliminate disagreements among local estimates. The optimal and sub-optimal consensus KF proposed in [7] was proven to be Lyapunov stable. Similarly, the Kullback–Leibler average was adopted for distributed consensus estimation [8]. Compared with consensus KF, the incremental step of diffusion KF [9] exchanges the measurements between neighbours, to generate intermediate estimates,

which leads to an additional enhancement in tracking performance. In [10], a diffusion KF with covariance intersection (CI) was developed, to overcome unknown cross-correlations. In [11], a diffusion KF with intermittent measurements was proposed, to tackle the loss of the measurement packets. Furthermore, in order to address DSE for nonlinear systems, the well-known extended Kalman filter (EKF), unscented Kalman filter (UKF) [12], and cubature Kalman filter (CKF) [13] were introduced [14,15]. The consensus-based UKF was proposed in [16], replacing the measurement function with linear regression [17]. Accordingly, a diffusion UKF based on CI was proposed in [18] with similar techniques and with consideration of intermittent measurements and theoretical analysis in terms of performance. In addition, a diffusion CKF with packet loss was derived in [19].

Compared with the improvement of tracking accuracy with DSE algorithms, the geometry between UAVs and their target plays a fundamental role in determining the quality of the measurements, which directly influences the accuracy of target tracking systems [20,21]. The Fisher information matrix (FIM) is a commonly used criterion assessing the quantity of information from measurements. The inverse of the FIM, called Cramer–Rao lower bound (CRLB), indicates the optimal performance of a tracking system. The optimal sensor–target geometry was obtained by optimizing the functions related to the FIM for TOA, AOA, and hybrid sensors in 2D and 3D space [22–27]. In [28], a motion coordination algorithm was proposed for reconfiguration of the sensor–target geometry, based on the previous optimal sensor–target geometry. Model predicted control was adopted to achieve the optimal geometry for multiple-target localization in [29]. On the other hand, path optimization based on numerical methods has been proposed for target tracking, to avoid the difficulty of finding closed-form solutions [30–36]. In [37–39], gradient descent optimization algorithms were proposed for single- and multi-sensor path planning for AOA target tracking, by minimizing the trace of the error covariance in 2D and 3D space. In [40], path optimization for passive emitter localization in 2D space was transformed into a nonlinear programming problem, to minimize the determinant of the FIM. In [41], a trajectory optimization method was proposed through maximizing the geometrical observability metric with bearings-only measurement. Path optimization for multi-target tracking, by minimizing the predicted conditional CRLB, was studied in [42], using a non-convex optimization method.

In general, the evolution of DSE algorithms and path optimization for UAVs provides improved performance for target tracking. In practical applications, due to intricate environments, the failure of detection and communication of UAVs leads to intermittent measurements [11,18]. Moreover, the cross-correlation between estimates is crucial for ensuring a consistent fusion estimate; however, this is difficult to calculate. The CKF has been verified to have a better tracking accuracy compared with EKF and UKF in high dimension nonlinear systems, and the diffusion strategy guarantees an improved estimation accuracy by exchanging local information. Nevertheless, few studies have taken intermittent measurements and unknown cross-correlations into account in a diffusion CKF. On the other hand, the majority of existing distributed path optimization methods for enhancing tracking performance primarily consider functions related to the local error covariance matrix as optimization objectives. While these methods effectively improve tracking performance, they can potentially lead to a decrease in the local estimation accuracy within the system, as a penalty. Therefore, inspired by distributed optimization for multiple agents [43–46], the local estimation of other agents by each agent for optimal solutions has a great impact on the optimization problem, with the cost function as the sum of the local functions. However, most existing works did not take the location of the neighboring UAVs into consideration for distributed UAV path optimization, which may lead to local optima and even divergences.

Motivated by the aforementioned considerations, this paper focuses on distributed state estimation and UAV path optimization for target tracking. A diffusion CKF algorithm for target tracking is studied. Meanwhile, distributed path optimization is considered, to improve the tracking performance of the whole system. The contributions of this paper are as follows:

- i A diffusion CKF with intermittent measurements based on CI (DCKFI-CI) is proposed, under consideration of detection failure and unknown correlations, which were not fully taken into account for diffusion CKF in previous studies. Moreover, its information-based form is derived by leveraging a pseudo measurement matrix;
- ii The consistency and bounded error covariance of the diffusion estimate are analyzed theoretically, to demonstrate the performance of the proposed DCKFI-CI. The previous results of bounded error covariance were based on strong assumptions about detection probability. In this paper, the condition of the bounded error covariance is also derived;
- iii A distributed path optimization method is developed by minimizing the sum of the traces of the fusion error covariance matrices; instead of the local error covariance for each UAV used in previous works. Based on exchanging the local estimate of the optimal solution, the cost function is minimized, which improves the accuracy of the whole tracking system.

The remainder of this paper is organized as follows: Section 2 presents the problem formulation. In Section 3, we propose the DCKFI-CI algorithm and derive its information-based form. Section 4 presents a performance analysis of the DCKFI-CI algorithm. In Section 5, we design a path optimization strategy. The proposed method is verified using simulation in Section 6. Section 7 concludes the paper.

**Notation:** The 2-norm of a vector  $x \in \mathbb{R}^n$  is defined as  $\|x\| = \sqrt{x^T x}$ .  $\text{tr}(A)$  denotes the trace of the matrix  $A$ .  $\text{Chol}(A)$  denotes the Cholesky decomposition of  $A$ .  $|S|$  denote the cardinality of the set  $S$ .  $S \setminus T = \{e | e \in S \text{ and } e \notin T\}$ .  $\mathbb{E}\{x\}$  denotes the mathematical expectation of the stochastic variable  $x$ .

## 2. Problem Formulation

In this paper, we focus on the target tracking problem of multiple cooperative UAVs in 3D space, as depicted in Figure 1. UAVs are equipped with detection sensors, communication units, and data processors. However, due to detection failure, the measurements taken by UAVs are unfortunately intermittent. The state of the target is estimated by the data processor by incorporating these intermittent measurements and information shared among wireless-connected UAVs through their communication units. In addition, UAVs possess the capability to engage in coordinated movement, to perform the task of target tracking.

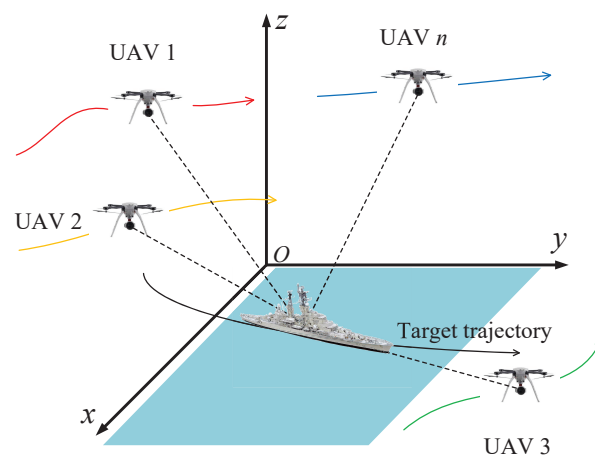


**Figure 1.** Target tracking with multiple UAVs.

As shown in Figure 1, we consider a typical scenario in practical target tracking applications. The target motion and intermittent measurements are modeled as a nonlinear discrete system

$$\begin{aligned} \mathbf{x}_{k+1} &= f(\mathbf{x}_k) + \mathbf{w}_k \\ z_k^i &= \gamma_k^i h^i(\mathbf{x}_k) + \eta_k^i \end{aligned} \quad (1)$$

where  $\mathbf{x}_k \in \mathbb{R}^{n_x}$  is the state vector of the target at time  $k$ ;  $\mathbf{z}_k^i \in \mathbb{R}^{n_z}$  is the measurement vector detected by the sensor equipped on the  $i$ th UAV at time  $k$ ;  $f(\cdot)$  and  $h^i(\cdot)$  denote the process and measurement function; the process noise  $\mathbf{w}_k \in \mathbb{R}^{n_x}$  and the measurement noise  $\boldsymbol{\eta}_k^i \in \mathbb{R}^{n_z}$  are mutually uncorrected Gaussian noise with zero mean and covariance  $\mathbf{Q}_k$  and  $\mathbf{R}_k^i$ , respectively;  $n_x$  and  $n_z$  are the dimensions of the state and measurement vectors, respectively; and  $\gamma_k^i$  is a binary stochastic variable to describe the intermittent measurement model, i.e.,  $\gamma_k^i = 0$  or  $1$  indicates that the measurement of the  $i$ th UAV is missing or not at time  $k$ , respectively. The probability distribution of  $\gamma_k^i$  is

$$\begin{cases} \mathbb{P}\{\gamma_k^i = 1\} = \lambda_i \\ \mathbb{P}\{\gamma_k^i = 0\} = 1 - \lambda_i \end{cases} \quad (2)$$

where  $\lambda_i$  represents the detection probability with  $0 \leq \lambda_i \leq 1$ , then the measurement noise follows

$$\mathbb{P}(\boldsymbol{\eta}_k^i | \gamma_k^i) = \begin{cases} \mathcal{N}(\mathbf{0}, \mathbf{R}_k^i) & \gamma_k^i = 1 \\ \mathcal{N}(\mathbf{0}, \sigma^2 \mathbf{I}) & \gamma_k^i = 0 \end{cases} \quad (3)$$

where  $\mathcal{N}(\cdot, \cdot)$  denotes the norm distribution, and the absence of measurement leads to a limiting case of  $\sigma \rightarrow \infty$ .

The communication topology among UAVs in this paper is described as a time-invariant undirected graph  $\mathcal{G} = (\mathcal{N}, \mathcal{E})$ , where  $\mathcal{N} = \{1, 2, \dots, n\}$  is the vertex set, and  $\mathcal{E} \subset \mathcal{N} \times \mathcal{N}$  is the edge set. Moreover,  $(i, j) \in \mathcal{E}$  ( $i \neq j$ ) means that the  $i$ th UAV and the  $j$ th UAV can communicate with each other directly; that is, the  $j$ th UAV is a neighbor of the  $i$ th UAV.  $\mathcal{N}_i = \{j | (i, j) \in \mathcal{E}\} \cup i$  denotes the set of UAVs that are connected to the  $i$ th UAV and itself.

The motion model of the UAVs is given by

$$\mathbf{s}_i(k+1) = \mathbf{s}_i(k) + \mathbf{u}_i(k) \quad (4)$$

where  $\mathbf{s}_i(k) = [s_{ix}(k), s_{iy}(k), s_{iz}(k)]^T \in \mathbb{R}^3$  is the position of the  $i$ th UAV at time  $k$ ; and  $\mathbf{u}_i(k)$  is the control input vector of the  $i$ th UAV at time  $k$ .

The state parameters of the target are unknown. It is assumed that the location of the UAVs and the measurements taken by them are known to themselves. Taking into account the communication bandwidth, only limited information can be transmitted between the UAVs, in accordance with the communication topology. Our objective is to estimate the target's state using intermittent measurements and improve the tracking accuracy by optimizing the path for the cooperation of the UAVs.

### 3. Diffusion CKF Based on a Covariance Intersection with Intermittent Measurements

In this section, a diffusion CKF is proposed for the distributed estimation with intermittent measurements taken by the UAVs. In addition, a covariance intersection is introduced to address the unknown cross-correlations of the target tracking system. We first derive the time- and measurement-updated form of DCKFI-CI based on the local CKF with the intermittent measurements. Then, we transform this into an information-based form by introducing a pseudo measurement matrix.

#### 3.1. Local CKF with Intermittent Measurements

Before we derive the diffusion framework, the local CKF with intermittent measurements is briefly reviewed. Denote  $\hat{\mathbf{x}}_{k|k}^i$  as the local estimate of  $\mathbf{x}_k$  and  $\mathbf{P}_{k|k}^i$  as the estimate error covariance matrix for the  $i$ th UAV. A local CKF with intermittent measurements for the  $i$ th UAV in its time- and measurement-updated forms can be computed by starting from  $\hat{\mathbf{x}}_{0|0}^i$  and  $\mathbf{P}_{0|0}^i$  [19]. The iteration functions are as follows:

Step 1. Evaluate cubature points ( $g = 1, 2, \dots, 2n_x$ )

$$S_{k-1|k-1}^i = \text{Chol}(P_{k-1|k-1}^i) \tag{5}$$

$$X_{g,k-1|k-1}^i = S_{k-1|k-1}^i \xi_g + \hat{x}_{k-1|k-1}^i, \quad g = 1, 2, \dots, 2n_x \tag{6}$$

where  $\xi_g = \sqrt{n_x}[1]_g; [1]_g \in R^{n_x}$  represents the  $g$ th element of the following set:

$$\underbrace{\left\{ \begin{bmatrix} 1 \\ 0 \\ \vdots \\ 0 \end{bmatrix}, \begin{bmatrix} 0 \\ 1 \\ \vdots \\ 0 \end{bmatrix}, \dots, \begin{bmatrix} 0 \\ 0 \\ \vdots \\ 1 \end{bmatrix}, \begin{bmatrix} -1 \\ 0 \\ \vdots \\ 0 \end{bmatrix}, \begin{bmatrix} 0 \\ -1 \\ \vdots \\ 0 \end{bmatrix}, \dots, \begin{bmatrix} 0 \\ 0 \\ \vdots \\ -1 \end{bmatrix} \right\}}_{2n_x}$$

Step 2. Time update

$$X_{g,k|k-1}^i = f(X_{g,k-1|k-1}^i), \quad g = 1, 2, \dots, 2n_x \tag{7}$$

$$\hat{x}_{k|k-1}^i = \frac{1}{2n_x} \sum_{g=1}^{2n_x} \chi_{g,k|k-1}^i \tag{8}$$

$$P_{k|k-1}^i = \frac{1}{2n_x} \sum_{g=1}^{2n_x} \chi_{g,k|k-1}^i (\chi_{g,k|k-1}^i)^T - \hat{x}_{k|k-1}^i (\hat{x}_{k|k-1}^i)^T + Q_{k-1} \tag{9}$$

Step 3. Measurement update

$$S_{k|k-1}^i = \text{Chol}(P_{k|k-1}^i) \tag{10}$$

$$X_{g,k|k-1}^i = S_{k|k-1}^i \xi_g + \hat{x}_{k|k-1}^i, \quad g = 1, 2, \dots, 2n_x \tag{11}$$

$$Z_{g,k|k-1}^i = h^i(\chi_{g,k|k-1}^i), \quad g = 1, 2, \dots, 2n_x \tag{12}$$

$$\hat{z}_{k|k-1}^i = \frac{1}{2n_x} \sum_{g=1}^{2n_x} Z_{g,k|k-1}^i \tag{13}$$

$$P_{zz,k|k-1}^i = \frac{1}{2n_x} \sum_{g=1}^{2n_x} Z_{g,k|k-1}^i (Z_{g,k|k-1}^i)^T - \hat{z}_{k|k-1}^i (\hat{z}_{k|k-1}^i)^T + R_k^i \tag{14}$$

$$P_{xz,k|k-1}^i = \frac{1}{2n_x} \sum_{g=1}^{2n_x} \chi_{g,k|k-1}^i (Z_{g,k|k-1}^i)^T - \hat{x}_{k|k-1}^i (\hat{z}_{k|k-1}^i)^T \tag{15}$$

$$M_k^i = P_{xz,k|k-1}^i (P_{zz,k|k-1}^i + (1 - \gamma_k^i) R_k^i + \gamma_k^i \sigma^2 I_{n_z})^{-1} \tag{16}$$

$$\hat{x}_{k|k}^i = \hat{x}_{k|k-1}^i + M_k^i (z_k^i - \hat{z}_{k|k-1}^i) \tag{17}$$

$$P_{k|k}^i = P_{k|k-1}^i - M_k^i P_{zz,k|k-1}^i (M_k^i)^T \tag{18}$$

Taking the limit as  $\sigma \rightarrow \infty$ , the Equations (16)–(18) can be rewritten as

$$\widetilde{M}_k^i = P_{xz,k|k-1}^i (P_{zz,k|k-1}^i)^{-1} \tag{19}$$

$$\hat{x}_{k|k}^i = \hat{x}_{k|k-1}^i + \gamma_k^i \widetilde{M}_k^i (z_k^i - \hat{z}_{k|k-1}^i) \tag{20}$$

$$P_{k|k}^i = P_{k|k-1}^i - \gamma_k^i \widetilde{M}_k^i P_{zz,k|k-1}^i (\widetilde{M}_k^i)^T \tag{21}$$

### 3.2. Diffusion Cubature Kalman Filter with Intermittent Measurements Based on CI

In this section, a DCKFI-CI is proposed based on the diffusion framework. Meanwhile, a covariance intersection is adopted, to address the unknown cross-correlations in the target tracking system.

First, a weighting mixing matrix is required for the diffusion update, whose elements represent the weights used to fuse the local estimates and error covariance matrices among neighbours in the diffusion strategy. The diffusion matrix  $C = [c_{ij}] \in \mathbb{R}^{n \times n}$  satisfies  $C\mathbf{1} = \mathbf{1}$ ,  $c_{ij} > 0$  if  $j \notin \mathcal{N}_i$ ,  $c_{ij} \geq 0$ . In this paper, the well-known Metropolis weights rule is adopted:

$$c_{ij} = \begin{cases} 1/(1 + \max\{d_i, d_j\}) & \text{if } (j, i) \in \mathcal{E} \\ 0 & \text{if } (j, i) \notin \mathcal{E} \text{ and } j \neq i \\ 1 - \sum_{l \in \mathcal{N}_i} c_{il} & \text{if } j = i \end{cases} \quad (22)$$

A DCKFI-CI algorithm is proposed by adding an incremental step for exchanging measurements among neighbours for local estimates and a diffusion step based on CI. As the  $i$ th UAV can obtain its neighbours' measurements, let  $\mathcal{N}_i = \{i_1, i_2, \dots, i_{\mathcal{N}_i}\}$ , then the augmented measurement vector for the  $i$ th UAV and its corresponding measurement noise covariance matrix are

$$\mathbf{z}_k^i = \left[ \left( z_k^{i_1} \right)^T, \left( z_k^{i_2} \right)^T, \dots, \left( z_k^{i_{\mathcal{N}_i}} \right)^T \right]^T = \check{h}^i(x_k^i) \quad (23)$$

$$\check{\mathbf{R}}_k^i = \text{diag} \left\{ \mathbf{R}_k^{i_1}, \mathbf{R}_k^{i_2}, \dots, \mathbf{R}_k^{i_{\mathcal{N}_i}} \right\} \quad (24)$$

$$\check{\gamma}_k^i = \text{diag} \left\{ \gamma_k^{i_1} \mathbf{I}_{n_z}, \gamma_k^{i_2} \mathbf{I}_{n_z}, \dots, \gamma_k^{i_{\mathcal{N}_i}} \mathbf{I}_{n_z} \right\} \quad (25)$$

Thus, a DCKFI-CI algorithm with time- and measurement-update is presented in Algorithm 1.

An alternative transformation for Algorithm 1 would be replacing the measurement-update form with the information form for CKFI in the incremental update. Accordingly, a pseudo measurement matrix is introduced, which was also seen in [16–18], to facilitate obtaining the applicable information form in the diffusion framework, which is defined by

$$\mathcal{H}_k^i = \left( \mathbf{P}_{xz,k|k-1}^i \right)^T \left( \mathbf{P}_{k|k-1}^i \right)^{-1} \quad (26)$$

Combining (19), (21) and (26) and according to matrix inversion lemma, we have

$$\left( \mathbf{P}_{k|k}^i \right)^{-1} = \left( \mathbf{P}_{k|k-1}^i \right)^{-1} + \gamma_k^i \left( \mathcal{H}_k^i \right)^T \left( \mathcal{R}_k^i \right)^{-1} \mathcal{H}_k^i \quad (27)$$

where

$$\mathcal{R}_k^i = \mathbf{P}_{zz,k|k-1}^i - \mathcal{H}_k^i \mathbf{P}_{xz,k|k-1}^i \quad (28)$$

---

**Algorithm 1** DCKFI-CI (Time- and measurement-update)

---

**Input:**  $\hat{x}_{0,f}^i, P_{0,f}^i, z_k^i, R_k^i, Q_{k-1}, i \in \mathcal{N}$

**Output:**  $\hat{x}_{k,f}^i, P_{k,f}^i$

1: Initialization

Consider a nonlinear model as in (1). Start with  $\hat{x}_{0|0}^i = \hat{x}_{0,f}^i$  and  $P_{0|0}^i = P_{0,f}^i$ .

2: Evaluating cubature points and time-update steps follows the local CKF with intermittent measurements in Section 3.1.

3: Collect the measurements from  $\mathcal{N}_i$

4: Measurement update

$$S_{k|k-1}^i = \text{Chol}(P_{k|k-1}^i)$$

$$\chi_{g,k|k-1}^i = S_{k|k-1}^i \tilde{\zeta}_g + \hat{x}_{k|k-1}^i, g = 1, 2, \dots, 2n_x$$

$$Z_{g,k|k-1}^i = \check{h}^i(\chi_{g,k|k-1}^i), g = 1, 2, \dots, 2n_x$$

$$\hat{z}_{k|k-1}^i = \frac{1}{2n_x} \sum_{g=1}^{2n_x} Z_{g,k|k-1}^i$$

$$P_{zz,k|k-1}^i = \frac{1}{2n_x} \sum_{g=1}^{2n_x} Z_{g,k|k-1}^i (Z_{g,k|k-1}^i)^T - \hat{z}_{k|k-1}^i (\hat{z}_{k|k-1}^i)^T + \check{R}_k^i$$

$$P_{xz,k|k-1}^i = \frac{1}{2n_x} \sum_{g=1}^{2n_x} \chi_{g,k|k-1}^i (Z_{g,k|k-1}^i)^T - \hat{x}_{k|k-1}^i (\hat{z}_{k|k-1}^i)^T$$

$$M_k^i = P_{xz,k|k-1}^i \left( P_{zz,k|k-1}^i + (I_{n_z \parallel \mathcal{N}_i} - \check{\gamma}_k^i) \check{R}_k^i + \sigma^2 \check{\gamma}_k^i I_{n_z \parallel \mathcal{N}_i} \right)^{-1}$$

$$x_{k,inc}^i = x_{k|k-1}^i + M_k^i (z_k^i - \hat{z}_{k|k-1}^i)$$

$$P_{k,inc}^i = P_{k|k-1}^i - M_k^i P_{zz,k|k-1}^i (M_k^i)^T$$

5: Propagate  $\hat{x}_{k,inc}^i$  and  $P_{k,inc}^i$  to their neighbours  $\mathcal{N}_i \setminus i$

6: Diffusion update with CI

$$(P_{k,f}^i)^{-1} = \sum_{j \in \mathcal{N}_i} c_{ij} (P_{k,inc}^j)^{-1}$$

$$\hat{x}_{k,f}^i = P_{k,f}^i \sum_{j \in \mathcal{N}_i} c_{ij} (P_{k,inc}^j)^{-1} \hat{x}_{k,inc}^j$$


---

Thus, the DCKFI-CI in the information form is presented in Algorithm 2.

---

**Algorithm 2** DCKFI-CI (Information form)

---

**Input:**  $\hat{x}_{0,f}^i, P_{0,f}^i, z_k^i, R_k^i, Q_{k-1}, i \in \mathcal{N}$

**Output:**  $\hat{x}_{k,f}^i, P_{k,f}^i$

1: Initialization

Consider a nonlinear model as in (1). Start with  $\hat{x}_{0|0}^i = \hat{x}_{0,f}^i$  and  $P_{0|0}^i = P_{0,f}^i, i = 1, 2, \dots, n$ .

2: Evaluating cubature points and prediction steps follow the local CKF with intermittent measurements in Section 3.1.

3: Calculate  $\mathcal{H}_k^i$  and  $\mathcal{R}_k^i$  through (10)–(15), (26) and (28)

4: Propagate  $\mathcal{H}_k^i, \mathcal{R}_k^i$  and  $z_k^i$  to their neighbours  $\mathcal{N}_i \setminus i$

5: Information update

$$\begin{aligned}
 Y_k^i &= \sum_{j \in \mathcal{N}_i} \gamma_k^j (\mathcal{H}_k^j)^T (\mathcal{R}_k^j)^{-1} \mathcal{H}_k^j \\
 q_k^i &= \sum_{j \in \mathcal{N}_i} \gamma_k^j (\mathcal{H}_k^j)^T (\mathcal{R}_k^j)^{-1} z_k^j \\
 (P_{k,inc}^i)^{-1} &= (P_{k|k-1}^i)^{-1} + Y_k^i \\
 \hat{x}_{k,inc}^i &= \hat{x}_{k|k-1}^i + P_{k,inc}^i (q_k^i - Y_k^i \hat{x}_{k|k-1}^i)
 \end{aligned}$$

6: Propagate  $\hat{x}_{k,inc}^i$  and  $P_{k,inc}^i$  to their neighbours  $\mathcal{N}_i \setminus i$

7: Diffusion update with CI

$$\begin{aligned}
 (P_{k,f}^i)^{-1} &= \sum_{j \in \mathcal{N}_i} c_{ij} (P_{k,inc}^j)^{-1} \\
 \hat{x}_{k,f}^i &= P_{k,f}^i \sum_{j \in \mathcal{N}_i} c_{ij} (P_{k,inc}^j)^{-1} \hat{x}_{k,inc}^j
 \end{aligned}$$


---

**Remark 1.** The pseudo measurement matrix in (26) is a linear regression of the nonlinear measurement function [17]. Similarly,  $\mathcal{H}_k^i$  can be alternatively approximated by the first order Taylor series expansion matrix at  $\hat{x}_{k|k-1}$ .

#### 4. Performance Analysis

In this section, the performance of the DCKFI-CI algorithm based on the information form is analyzed. The consistency of the fusion estimate is analyzed, to evaluate the fusion performance of the DCKFI-CI. In addition, the trace of the error covariance matrix is proven to be bounded under a certain condition of the detection probability.

Define the estimated error and innovation, respectively, as

$$\begin{cases} \hat{x}_{k|k-1}^i = x_k - \hat{x}_{k|k-1}^i \\ \hat{z}_{k|k-1}^i = z_k^i - \hat{z}_{k|k-1}^i \end{cases} \tag{29}$$

The equations in (29) can be rewritten in a pseudo linearized form as

$$\begin{cases} \hat{x}_{k|k-1}^i = \alpha_{k-1}^i F_{k-1}^i (x_{k-1} - \hat{x}_{k-1,f}^i) + w_{k-1} \\ \hat{z}_k^i = \gamma_k^i \beta_k^i H_k^i (x_{k-1} - \hat{x}_{k-1,f}^i) + \eta_k^i \end{cases} \tag{30}$$

where  $F_{k-1}^i = \frac{\partial f(x_{k-1})}{\partial x_{k-1}} \Big|_{\hat{x}_{k-1,f}^i}$  and  $H_k^i = \frac{\partial h^i(x_k)}{\partial x_{k-1}} \Big|_{\hat{x}_{k,f}^i}$  are the first-order Taylor series expansion of the state transformation and measurement functions, respectively;  $\alpha_{k-1}^i =$

$\text{diag}(\alpha_{1,k-1}^i \alpha_{2,k-1}^i \cdots \alpha_{n_x,k-1}^i)$  and  $\beta_{k-1}^i = \text{diag}(\beta_{1,k-1}^i \beta_{2,k-1}^i \cdots \beta_{n_z,k-1}^i)$  are the compensation instrumental diagonal matrices used to adjust the approximation error of the pseudo linearized state system and measurement matrices.

Substituting (30) into the formulas in CKFI, we obtain

$$P_{k|k-1}^i = \alpha_{k-1}^i F_{k-1}^i P_{k-1,f}^i (F_{k-1}^i)^T \alpha_{k-1}^i + Q_{k-1}^* \tag{31}$$

where  $Q_{k-1}^* = Q_{k-1} + \mu P_{k|k-1}^i + \kappa P_{k|k-1}^i$  is positive definite,  $\mu P_{k|k-1}^i$  is the difference between  $\alpha_{k-1}^i F_{k-1}^i P_{k-1,f}^i (F_{k-1}^i)^T \alpha_{k-1}^i$ , and  $\mathbb{E} \left\{ \alpha_{k-1}^i F_{k-1}^i P_{k-1,f}^i (F_{k-1}^i)^T \alpha_{k-1}^i \right\}$ ,  $\kappa P_{k|k-1}^i$  is the difference between the real error covariance matrix and the estimated error covariance matrix. In order to compensate for the approximation error of the pseudo measurement matrix, a stochastic matrix  $\Phi_k^i \in \mathbb{R}^{n_x \times n_x}$  is introduced [47], so we have

$$\mathcal{H}_k^i = (P_{xz,k|k-1}^i)^T (P_{k|k-1}^i)^{-1} = \beta_k^i H_k^i \Phi_k^i \tag{32}$$

Then, the related formulas of DCKFI-CI in information form can be rewritten as

$$Y_k^i = \sum_{j \in \mathcal{N}_i} \gamma_k^j (\beta_k^j H_k^j \Phi_k^j)^T (R_k^j)^{-1} \beta_k^j H_k^j \Phi_k^j \tag{33}$$

$$q_k^i = \sum_{j \in \mathcal{N}_i} \gamma_k^j (\beta_k^j H_k^j \Phi_k^j)^T (R_k^j)^{-1} z_k^j \tag{34}$$

**Definition 1** ([48]). Let  $\hat{x}$  represent an unbiased estimate of an unknown stochastic vector  $x$ ;  $P$  and  $\check{P}$  denote the estimated and real error covariance matrices, respectively. The estimate  $\hat{x}$  is referred to as a consistent estimate of  $x$  if  $P \geq \check{P} = \mathbb{E}\{(x - \hat{x})(x - \hat{x})^T\}$ .

**Theorem 1.** The fusion estimate obtained by DCKFI-CI is a consistent estimate, i.e.,  $P_{k,f}^i \geq \check{P}_{k,f}^i = \mathbb{E}\{(x - \hat{x}_{k,f}^i)(x - \hat{x}_{k,f}^i)^T\}$ .

**Proof.** The proof is proceeded using the method of induction. Suppose that  $P_{k-1,f}^i \geq \check{P}_{k-1,f}^i$  holds at time  $k - 1$ ,  $\check{P}_{k|k-1}^i$  is derived as

$$\begin{aligned} \check{P}_{k|k-1}^i &= \mathbb{E} \left\{ (x_k - \hat{x}_{k|k-1}^i) (x_k - \hat{x}_{k|k-1}^i)^T \right\} \\ &= \mathbb{E} \left\{ (\alpha_{k-1}^i F_{k-1}^i (x_{k-1} - \hat{x}_{k-1,f}^i) + w_{k-1}) (\alpha_{k-1}^i F_{k-1}^i (x_{k-1} - \hat{x}_{k-1,f}^i) + w_{k-1})^T \right\} \\ &= \alpha_{k-1}^i F_{k-1}^i \check{P}_{k-1,f}^i (\alpha_{k-1}^i F_{k-1}^i)^T + \mu P_{k|k-1}^i + Q_{k-1}^* \end{aligned} \tag{35}$$

Applying  $P_{k-1,f}^i \geq \check{P}_{k-1,f}^i$  into (35), we obtain

$$P_{k|k-1}^i \geq \alpha_{k-1}^i F_{k-1}^i \check{P}_{k-1,f}^i (\alpha_{k-1}^i F_{k-1}^i)^T + Q_{k-1}^* \geq \check{P}_{k|k-1}^i \tag{36}$$

Next, we consider the real error covariance matrix  $\check{P}_{k,inc}^i$  in the step of information updating

$$\begin{aligned}
 \check{P}_{k,inc}^i &= \mathbb{E} \left\{ \left( \mathbf{x}_k - \hat{\mathbf{x}}_{k,inc}^i \right) \left( \mathbf{x}_k - \hat{\mathbf{x}}_{k,inc}^i \right)^T \right\} \\
 &= \mathbb{E} \left\{ \left[ \left( \mathbf{I} - \mathbf{P}_{k,inc}^i \mathbf{Y}_k^i \right) \hat{\mathbf{x}}_{k|k-1}^i \right] \left[ \left( \mathbf{I} - \mathbf{P}_{k,inc}^i \mathbf{Y}_k^i \right) \hat{\mathbf{x}}_{k|k-1}^i \right]^T \right. \\
 &\quad \left. + \left[ \mathbf{P}_{k,inc}^i \sum_{j \in \mathcal{N}_i} \gamma_k^j \left( \boldsymbol{\beta}_k^j \mathbf{H}_k^j \boldsymbol{\Phi}_k^i \right)^T \left( \mathbf{R}_k^j \right)^{-1} \boldsymbol{\eta}_k^j \right] \right. \\
 &\quad \left. \left[ \mathbf{P}_{k,inc}^i \sum_{j \in \mathcal{N}_i} \gamma_k^j \left( \boldsymbol{\beta}_k^j \mathbf{H}_k^j \boldsymbol{\Phi}_k^i \right)^T \left( \mathbf{R}_k^j \right)^{-1} \boldsymbol{\eta}_k^j \right]^T \right\} \tag{37}
 \end{aligned}$$

where  $\hat{\mathbf{x}}_{k|k-1}^i = \mathbf{x}_k - \hat{\mathbf{x}}_{k|k-1}^i$ . Due to  $\mathbb{E}[\boldsymbol{\eta}_k^i(\boldsymbol{\eta}_k^i)^T] = \mathbf{R}_k^i$  and  $\mathbb{E}[\boldsymbol{\eta}_k^i(\boldsymbol{\eta}_k^j)^T] = \mathbf{0}$ ,  $i \neq j$ , it follows that

$$\begin{aligned}
 &\mathbb{E} \left\{ \left[ \mathbf{P}_{k,inc}^i \sum_{j \in \mathcal{N}_i} \gamma_k^j \left( \boldsymbol{\beta}_k^j \mathbf{H}_k^j \boldsymbol{\Phi}_k^i \right)^T \left( \mathbf{R}_k^j \right)^{-1} \boldsymbol{\eta}_k^j \right] \left[ \mathbf{P}_{k,inc}^i \sum_{j \in \mathcal{N}_i} \gamma_k^j \left( \boldsymbol{\beta}_k^j \mathbf{H}_k^j \boldsymbol{\Phi}_k^i \right)^T \left( \mathbf{R}_k^j \right)^{-1} \boldsymbol{\eta}_k^j \right]^T \right\} \\
 &= \mathbb{E} \left\{ \mathbf{P}_{k,inc}^i \left[ \sum_{j \in \mathcal{N}_i} \left( \gamma_k^j \right)^2 \left( \boldsymbol{\beta}_k^j \mathbf{H}_k^j \boldsymbol{\Phi}_k^i \right)^T \left( \mathbf{R}_k^j \right)^{-1} \boldsymbol{\beta}_k^j \mathbf{H}_k^j \boldsymbol{\Phi}_k^i \right] \mathbf{P}_{k,inc}^i \right\} = \mathbb{E} \left\{ \mathbf{P}_{k,inc}^i \mathbf{Y}_k^i \mathbf{P}_{k,inc}^i \right\} \tag{38}
 \end{aligned}$$

Substituting (38) into (37), it follows that

$$\check{P}_{k,inc}^i = \mathbb{E} \left\{ \left( \mathbf{I} - \mathbf{P}_{k,inc}^i \mathbf{Y}_k^i \right) \check{P}_{k|k-1}^i \left( \mathbf{I} - \mathbf{P}_{k,inc}^i \mathbf{Y}_k^i \right)^T + \mathbf{P}_{k,inc}^i \mathbf{Y}_k^i \mathbf{P}_{k,inc}^i \right\} \tag{39}$$

Multiplying  $\left( \mathbf{P}_{k,inc}^i \right)^{-1}$  on both sides of (38) and combining with (36), we obtain

$$\begin{aligned}
 \left( \mathbf{P}_{k,inc}^i \right)^{-1} \check{P}_{k,inc}^i &= \mathbb{E} \left\{ \left[ \left( \mathbf{P}_{k,inc}^i \right)^{-1} - \mathbf{Y}_k^i \right] \check{P}_{k|k-1}^i \left( \mathbf{I} - \mathbf{P}_{k,inc}^i \mathbf{Y}_k^i \right)^T + \mathbf{Y}_k^i \mathbf{P}_{k,inc}^i \right\} \\
 &= \mathbb{E} \left\{ \left( \mathbf{P}_{k|k-1}^i \right)^{-1} \check{P}_{k|k-1}^i \left( \mathbf{I} - \mathbf{P}_{k,inc}^i \mathbf{Y}_k^i \right)^T + \mathbf{Y}_k^i \mathbf{P}_{k,inc}^i \right\} \\
 &\leq \mathbb{E} \left\{ \left( \check{P}_{k|k-1}^i \right)^{-1} \check{P}_{k|k-1}^i \left( \mathbf{I} - \mathbf{P}_{k,inc}^i \mathbf{Y}_k^i \right)^T + \mathbf{Y}_k^i \mathbf{P}_{k,inc}^i \right\} \\
 &= \mathbb{E} \left\{ \mathbf{I} - \left( \mathbf{Y}_k^i \right)^T \left( \mathbf{P}_{k,inc}^i \right)^T + \mathbf{Y}_k^i \mathbf{P}_{k,inc}^i \right\} = \mathbf{I} \tag{40}
 \end{aligned}$$

In this case, we obtain  $\mathbf{P}_{k,inc}^i \geq \check{P}_{k,inc}^i$ , which indicates that the local estimate  $\hat{\mathbf{x}}_{k,inc}^i$  is a consistent estimate.

We now proceed to calculating the real fusion error covariance matrix  $\check{P}_{k,f}^i$  in the step of diffusion updating

$$\begin{aligned}
 \check{P}_{k,f}^i &= \mathbb{E} \left\{ \left( \mathbf{x}_k - \hat{\mathbf{x}}_{k,f}^i \right) \left( \mathbf{x}_k - \hat{\mathbf{x}}_{k,f}^i \right)^T \right\} \\
 &= \mathbf{P}_{k,f}^i \sum_{j=1}^n \sum_{l=1}^n c_{i,j} c_{i,l} \left( \mathbf{P}_{k,inc}^j \right)^{-1} \check{P}_{k,inc}^{j,l} \left( \mathbf{P}_{k,inc}^l \right)^{-1} \mathbf{P}_{k,f}^i \tag{41}
 \end{aligned}$$

where  $\check{P}_{k,inc}^{j,l} = \mathbb{E} \left\{ \hat{\mathbf{x}}_{k,inc}^j \left( \hat{\mathbf{x}}_{k,inc}^l \right)^T \right\}$ .

Define  $\Delta \mathbf{P}_{k,f}^i = \mathbf{P}_{k,f}^i - \check{P}_{k,f}^i$  then we need to prove  $\Delta \mathbf{P}_{k,f}^i \geq \mathbf{0}$

$$\begin{aligned}
 & \left(\mathbf{P}_{k,f}^i\right)^{-1} \Delta \mathbf{P}_{k,f}^i \left(\mathbf{P}_{k,f}^i\right)^{-1} \\
 &= \sum_{j=1}^n c_{ij} \left(\mathbf{P}_{k,inc}^j\right)^{-1} - \sum_{j=1}^n \sum_{l=1}^n c_{ij} c_{il} \left(\mathbf{P}_{k,inc}^j\right)^{-1} \check{\mathbf{P}}_{k,inc}^{jl} \left(\mathbf{P}_{k,inc}^j\right)^{-1} \\
 &\geq \sum_{j=1}^n c_{ij} \left(\mathbf{P}_{k,inc}^j\right)^{-1} \check{\mathbf{P}}_{k,inc}^j \left(\mathbf{P}_{k,inc}^j\right)^{-1} - \sum_{j=1}^n \sum_{l=1}^n c_{ij} c_{il} \left(\mathbf{P}_{k,inc}^j\right)^{-1} \check{\mathbf{P}}_{k,inc}^{j,l} \left(\mathbf{P}_{k,inc}^l\right)^{-1} \quad (42)
 \end{aligned}$$

Noting that  $\sum_{l=1, l \neq j}^n c_{il} = 1 - c_{ii}$ , (42) becomes

$$\begin{aligned}
 & \left(\mathbf{P}_{k,f}^i\right)^{-1} \Delta \mathbf{P}_{k,f}^i \left(\mathbf{P}_{k,f}^i\right)^{-1} \\
 &\geq \sum_{j=1}^n \sum_{l=1, l \neq j}^n c_{ij} c_{il} \left[ \left(\mathbf{P}_{k,inc}^j\right)^{-1} \check{\mathbf{P}}_{k,inc}^j \left(\mathbf{P}_{k,inc}^j\right)^{-1} - \left(\mathbf{P}_{k,inc}^j\right)^{-1} \check{\mathbf{P}}_{k,inc}^{jl} \left(\mathbf{P}_{k,inc}^l\right)^{-1} \right] \\
 &= \sum_{j=1}^n \sum_{l=j}^n c_{ij} c_{il} \left[ \left(\mathbf{P}_{k,inc}^j\right)^{-1} \check{\mathbf{P}}_{k,inc}^j \left(\mathbf{P}_{k,inc}^j\right)^{-1} - \left(\mathbf{P}_{k,inc}^j\right)^{-1} \check{\mathbf{P}}_{k,inc}^{jl} \left(\mathbf{P}_{k,inc}^l\right)^{-1} \right. \\
 &\quad \left. - \left(\mathbf{P}_{k,inc}^l\right)^{-1} \check{\mathbf{P}}_{k,inc}^{lj} \left(\mathbf{P}_{k,inc}^j\right)^{-1} + \left(\mathbf{P}_{k,inc}^l\right)^{-1} \check{\mathbf{P}}_{k,inc}^l \left(\mathbf{P}_{k,inc}^l\right)^{-1} \right] \\
 &= \sum_{j=1}^n \sum_{l=j+1}^n c_{i,j} c_{i,l} \mathbb{E} \left\{ \left( \left(\mathbf{P}_{k,inc}^j\right)^{-1} \check{\mathbf{x}}_{k,inc}^j - \left(\mathbf{P}_{k,inc}^l\right)^{-1} \check{\mathbf{x}}_{k,inc}^l \right) \right. \\
 &\quad \left. \left( \left(\mathbf{P}_{k,inc}^j\right)^{-1} \check{\mathbf{x}}_{k,inc}^j - \left(\mathbf{P}_{k,inc}^l\right)^{-1} \check{\mathbf{x}}_{k,inc}^l \right)^T \right\} \geq 0 \quad (43)
 \end{aligned}$$

Thus, we have  $\Delta \mathbf{P}_{k,f}^i \geq 0$ , i.e.,  $\mathbf{P}_{k,f}^i \geq \check{\mathbf{P}}_{k,f}^i$  and this completes the proof.  $\square$

**Lemma 1** ([47]). For symmetric positive definite matrix  $\mathbf{A}, \mathbf{B} \in \mathbb{R}^{n \times n}$ ,  $(\mathbf{A} + \mathbf{B})^{-1} > \mathbf{A}^{-1} - \mathbf{A}^{-1} \mathbf{B} \mathbf{A}^{-1}$ .

**Assumption 1** ([47]). There exist positive real constants  $\bar{f}, \bar{\alpha}, \bar{h}, \bar{\beta}, \bar{q}, \bar{r}, \bar{\phi} > 0$ , such that the following bounds on the system parameter matrices are satisfied

$$\begin{cases} \|\mathbf{F}_k\| \leq \bar{f}, \|\boldsymbol{\alpha}_k\| \leq \bar{\alpha} \\ \underline{h} \leq \|\mathbf{H}_k\|, \underline{\beta} \leq \|\boldsymbol{\beta}_k\|, \|\boldsymbol{\Phi}_k\| \leq \bar{\phi} \\ \mathbf{Q}_k^* \leq \bar{q} \mathbf{I}, \mathbf{R}_k \leq \bar{r} \mathbf{I} \end{cases} \quad (44)$$

**Theorem 2.** Suppose that Assumption 1 holds and the linear form of the system in (1) is uniformly observable, there exists a critical value  $\underline{\lambda} = 1 - \frac{\bar{a}^2 \bar{f}^2 - 1}{\bar{a}^2 \bar{f}^2 \bar{\phi}^2}$ , such that if  $\prod_{j \in \mathcal{N}_i} (1 - \lambda_j) \leq \underline{\lambda}$ , the following inequality holds

$$\mathbb{E} \left\{ \text{tr} \left( \mathbf{P}_{k,f}^i \right) \right\} \leq \mathbb{E} \left\{ \text{tr} \left( \mathbf{P}_{k,inc}^i \right) \right\} \leq \bar{p} \quad (45)$$

**Proof.** According to the step of diffusion updating in DCKFI-CI, we have

$$\begin{aligned}
 \left(\mathbf{P}_{k,f}^i\right)^{-1} &= \sum_{j \in \mathcal{N}_i} c_{ij} \left(\mathbf{P}_{k,inc}^j\right)^{-1} \\
 &= \sum_{j \in \mathcal{N}_i} c_{ij} \left[ \left(\mathbf{P}_{k|k-1}^j\right)^{-1} + \sum_{j \in \mathcal{N}_i} \gamma_k^j \left(\boldsymbol{\beta}_k^j \mathbf{H}_k^j \boldsymbol{\Phi}_k^j\right)^T \left(\mathbf{R}_k^j\right)^{-1} \boldsymbol{\beta}_k^j \mathbf{H}_k^j \boldsymbol{\Phi}_k^j \right] \quad (46)
 \end{aligned}$$

Since  $\gamma_k^i = 0$  or 1, so the following inequality holds

$$\left(\mathbf{P}_{k,f}^i\right)^{-1} \geq \sum_{j \in \mathcal{N}_i} c_{ij} \left(\mathbf{P}_{k|k-1}^j\right)^{-1} \tag{47}$$

Taking the trace of both sides, we obtain

$$\text{tr}\left(\mathbf{P}_{k,f}^i\right) \leq \text{tr}\left(\left[\sum_{j \in \mathcal{N}_i} c_{ij} \left(\mathbf{P}_{k|k-1}^j\right)^{-1}\right]^{-1}\right) \tag{48}$$

Without loss of generality, there exists  $j, l \in \mathcal{N}_i$ , such that  $c_{ij} = 1$  and  $c_{il} = 0, l \neq j$ ; then, we have

$$\text{tr}\left(\mathbf{P}_{k,f}^i\right) \leq \text{tr}\left(\mathbf{P}_{k|k-1}^j\right), \forall j \in \mathcal{N}_i \tag{49}$$

Substituting (31) into  $\text{tr}\left(\mathbf{P}_{k|k-1}^i\right)$ , we have

$$\begin{aligned} \text{tr}\left(\mathbf{P}_{k|k-1}^i\right) &= \text{tr}\left(\boldsymbol{\alpha}_{k-1}^i \mathbf{F}_{k-1}^i \mathbf{P}_{k-1,f}^i \left(\mathbf{F}_{k-1}^i\right)^T \boldsymbol{\alpha}_{k-1}^i + \mathbf{Q}_{k-1}^*\right) \\ &= \text{tr}\left(\boldsymbol{\alpha}_{k-1}^i \mathbf{F}_{k-1}^i \left(\sum_{j \in \mathcal{N}_i} c_{ij} \left(\mathbf{P}_{k-1,inc}^j\right)^{-1}\right)^{-1} \left(\mathbf{F}_{k-1}^i\right)^T \boldsymbol{\alpha}_{k-1}^i + \mathbf{Q}_{k-1}^*\right) \\ &\leq \text{tr}\left(\boldsymbol{\alpha}_{k-1}^i \mathbf{F}_{k-1}^i \mathbf{P}_{k-1,inc}^i \left(\mathbf{F}_{k-1}^i\right)^T \boldsymbol{\alpha}_{k-1}^i + \mathbf{Q}_{k-1}^*\right) \\ &= \text{tr}\left(\boldsymbol{\alpha}_{k-1}^i \mathbf{F}_{k-1}^i \left[\left(\mathbf{P}_{k-1|k-2}^i\right)^{-1} + \sum_{j \in \mathcal{N}_i} \gamma_{k-1}^j \left(\boldsymbol{\beta}_{k-1}^j \mathbf{H}_{k-1}^j \boldsymbol{\Phi}_{k-1}^i\right)^T \left(\mathbf{R}_{k-1}^j\right)^{-1}\right.\right. \\ &\quad \left.\left. \times \boldsymbol{\beta}_{k-1}^j \mathbf{H}_{k-1}^j \boldsymbol{\Phi}_{k-1}^i\right]^{-1} \left(\mathbf{F}_{k-1}^i\right)^T \boldsymbol{\alpha}_{k-1}^i + \mathbf{Q}_{k-1}^*\right) \end{aligned} \tag{50}$$

According to Lemma 1, we obtain

$$\begin{aligned} \text{tr}\left(\mathbf{P}_{k|k-1}^i\right) &\leq \text{tr}\left(\boldsymbol{\alpha}_{k-1}^i \mathbf{F}_{k-1}^i \mathbf{P}_{k-1|k-2}^i \left(\mathbf{F}_{k-1}^i\right)^T \boldsymbol{\alpha}_{k-1}^i + \mathbf{Q}_{k-1}^*\right) \\ &\quad - \gamma_k^i \boldsymbol{\alpha}_{k-1}^i \mathbf{F}_{k-1}^i \left(\boldsymbol{\Phi}_k^i\right)^T \mathbf{P}_{k-1|k-2}^i \boldsymbol{\Phi}_k^i \left(\mathbf{F}_{k-1}^i\right)^T \boldsymbol{\alpha}_{k-1}^i \\ &\quad + \gamma_k^i \boldsymbol{\alpha}_{k-1}^i \mathbf{F}_{k-1}^i \left(\boldsymbol{\Phi}_{k-1}^i\right)^T \left[\left(\boldsymbol{\beta}_{k-1}^i \mathbf{H}_{k-1}^i\right)^T\right]^{-1} \mathbf{R}_{k-1}^i \left(\boldsymbol{\beta}_{k-1}^i \mathbf{H}_{k-1}^i\right)^{-1} \boldsymbol{\Phi}_{k-1}^i \left(\mathbf{F}_{k-1}^i\right)^T \boldsymbol{\alpha}_{k-1}^i \end{aligned} \tag{51}$$

According to Assumption 1, we have

$$\text{tr}\left(\mathbf{P}_{k|k-1}^i\right) \leq \bar{\alpha}^2 \bar{f}^2 \left(1 - \gamma_k^i \bar{\phi}^2\right) \text{tr}\left(\mathbf{P}_{k-1|k-2}^i\right) + \left(\bar{q} + \gamma_k^i \frac{\bar{\alpha}^2 \bar{f}^2 \bar{\phi}^2 \bar{r}}{\underline{\beta}^2 \underline{h}^2}\right) n \tag{52}$$

Making recursion and taking the mathematical expectation of (52), we obtain

$$\begin{aligned} \mathbb{E}\left\{\text{tr}\left(\mathbf{P}_{k|k-1}^i\right)\right\} &\leq \left[\bar{\alpha}^2 \bar{f}^2 \left(1 - \bar{\phi}^2 \left(1 - \prod_{j \in \mathcal{N}_i} (1 - \lambda_j)\right)\right)\right]^k \text{tr}\left(\mathbf{P}_{1|0}\right) \\ &\quad + n \left(\bar{q} + \lambda_i \frac{\bar{\alpha}^2 \bar{f}^2 \bar{\phi}^2 r}{\underline{\beta}^2 \underline{h}^2}\right) \sum_{t=0}^{k-1} \left[\bar{\alpha}^2 \bar{f}^2 \left(1 - \bar{\phi}^2 \left(1 - \prod_{j \in \mathcal{N}_i} (1 - \lambda_j)\right)\right)\right]^t \end{aligned} \tag{53}$$

Denote

$$\bar{p} = \max \left\{ \text{tr} \{ \mathbf{P}_{1|0} \}, n \left( \bar{q} + \lambda_i \frac{\bar{\alpha}^2 \bar{f}^2 \bar{\phi}^2 - \bar{r}}{\beta^2 \underline{h}^2} \right) \right\} \tag{54}$$

Therefore, it is apparent that if  $\prod_{j \in \mathcal{N}_i} (1 - \lambda_j) \leq 1 - \frac{\bar{\alpha}^2 \bar{f}^2 - 1}{\bar{\alpha}^2 \bar{f}^2 \bar{\phi}^2}$ , it follows that

$$\mathbb{E} \left\{ \text{tr} \left( \mathbf{P}_{k,f}^i \right) \right\} \leq \mathbb{E} \left\{ \text{tr} \left( \mathbf{P}_{k|k-1}^i \right) \right\} \leq \bar{p} \tag{55}$$

and this completes the proof.  $\square$

### 5. Distributed Path Optimization

In this section, distributed UAV path optimization is considered, for the enhancement of the performance of the whole tracking system. As we know, the tracking performance of stationary detection platforms is theoretically bounded by the CRLB. Fortunately, the path optimization of UAVs, reconfiguring the geometry between the target and the UAVs, benefits the tracking performance. In the past, the trace of the local error covariance matrix was minimized without exchanging UAV positions, which lacks coordination. In this paper, the average of the traces of the error covariance matrices is minimized, to accomplish the improvement of the tracking performance for the entire network.

Define the cost function as

$$\min_{\epsilon(k)} J(\epsilon(k)) = \frac{1}{n} \sum_{i=1}^n J_i(\epsilon(k)) \tag{56}$$

where  $J_i(\epsilon_i(k)) = \text{tr}(\mathbf{P}_{k,f}^i)$  is the trace of the fused error covariance matrix and  $\epsilon(k) = [\hat{s}_1^T(k), \hat{s}_2^T(k), \dots, \hat{s}_n^T(k)]^T \in \mathbb{R}^{3n}$  is the augmented vector of the UAVs' positions.

To solve the optimization problem in (56), the  $i$ th UAV performs the following update rules [44]:

$$\begin{aligned} \epsilon_i(k+1) &= \sum_{j \in \mathcal{N}_i} w_{ij}(k) \epsilon_j(k) - \frac{v^T}{\|\mathbf{y}_i(k)\|} \mathbf{y}_i(k) \\ \mathbf{y}_i(k+1) &= \sum_{j \in \mathcal{N}_i} w_{ij}(k) \mathbf{y}_j(k) + \nabla J_i(\epsilon_i(k+1)) - \nabla J_i(\epsilon_i(k)) \end{aligned} \tag{57}$$

where  $\epsilon_i(k) = [\hat{s}_{i,1}^T(k), \hat{s}_{i,2}^T(k), \dots, \hat{s}_{i,n}^T(k)]^T$  is the local estimate of the  $i$ th UAV about the optimal solution at time  $k$ ;  $\mathbf{W} = [w_{ij}] \in \mathbb{R}^{n \times n}$  is the weighting mixing matrix, which can also be chosen according to the Metropolis weights rule;  $\nabla J_i(\cdot)$  is the gradient of the local objective function  $J_i(\cdot)$ ;  $v$  is the velocity of the UAV, which is assumed to be identical for each UAV.

The explicit expression for  $\nabla J_i(\epsilon_i(k))$  is difficult to derive, so we turn to numerical computation using a central finite difference approximation. Let

$$\nabla J_i(\epsilon_i(k)) = [\pi_1(k), \pi_2(k), \dots, \pi_{3n}(k)]^T \tag{58}$$

Then the  $l$ th elements of the gradient vector for the central finite difference approximation is given by

$$\pi_l(k) \approx \frac{J_i(\epsilon_i(k) + \delta_l) - J_i(\epsilon_i(k) - \delta_l)}{2\delta} \tag{59}$$

where  $\delta_l \in \mathbb{R}^{3n}$ ,  $l \in \{1, 2, \dots, 3n\}$  is a column vector consisting of zero entries, except for the  $l$ th entry, which is a small positive real constant, denoted as  $\delta$

$$\delta_l = [0, \dots, 0, \underbrace{\delta}_{l\text{th entry}}, 0, \dots, 0]^T \tag{60}$$

The accuracy of the gradient approximation depends on the chosen of  $\delta$ . A sufficiently small value of  $\delta$  helps avoid a large error. However, excessively small values may give rise to numerical issues.

To obtain  $J_i(\epsilon_i(k) \pm \delta_l)$ , updated error covariance matrices are required. We need a virtual position for the UAV, which moves from its current position by  $\pm\delta$  along a specific direction, and a virtual measurement of the fused target position is taken from the new UAV position. The virtual measurement, along with other real measurements, is utilized to perform estimation and fusion through DCKFI-CI, resulting in an updated error covariance matrix. The calculation process is presented in Algorithm 3, taking the  $j$ th UAV moving  $\delta$  along  $x$ -axis computed on the  $i$ th UAV as an example. The majority of the computational effort is dedicated to the numerical approximation of the gradient vector of the cost function, which requires repetitive invocations of DCKFI-CI.

---

**Algorithm 3** Calculation of  $J_i(\epsilon_i(k) + \delta_{3j-2})$  (Taking the  $j$ th UAV moving  $\delta$  along the  $x$ -axis as an example)

---

**Input:**  $\epsilon_i(k), \delta, \hat{x}_{k,f}^i$

**Output:**  $J_i(\epsilon_i(k) + \delta_{3j-2})$

- 1: Move the  $i$ th UAV to  $[s_{i,jx}(k) + \delta, s_{i,jy}(k), s_{i,jz}(k)]^T$
  - 2: Take the virtual measurement  $\hat{z}_k^j$  of  $\hat{x}_{k,f}^i$  from the new position
  - 3: Perform the DCKFI-CI with  $\hat{z}_k^j$  and  $\hat{z}_k^i$  ( $i \in \mathcal{N} \setminus j$ ) to obtain  $\hat{P}_{k,f}^i$
  - 4:  $J_i(\epsilon_i(k) + \delta_{3j-2}) = \text{tr}(\hat{P}_{k,f}^i)$
  - 5: **Return**  $J_i(\epsilon_i(k) + \delta_{3j-2})$
- 

The approximation of  $\nabla J_i(\epsilon_i(k))$  can be calculated using  $J_i(\epsilon_i(k) \pm \delta_l)$  and the recursion in (57) can be carried out. Therefore, the next waypoint of the  $i$ th UAV at time  $k + 1$  is

$$s_i(k + 1) = \hat{s}_{i,i}(k + 1) \tag{61}$$

where  $\hat{s}_{i,i}(k + 1)$  are the components of  $\epsilon_i(k + 1)$  calculated by (57).

**Remark 2.** Implementation of UAV collision avoidance is necessary when two UAVs come into close proximity. However, it is important to note that such an implementation may result in a decline in tracking performance [38,49,50]. Although advanced UAV collision avoidance strategies need to be contemplated, they exceed the scope of this paper.

## 6. Simulation Experiments

In this section, we illustrate the performance of the proposed algorithm with a typical simulation example. We consider the problem of tracking a maneuvering turning target using five UAVs equipped with AOA sensors in a 3D space. The communication topology among the UAVs is shown in Figure 2.

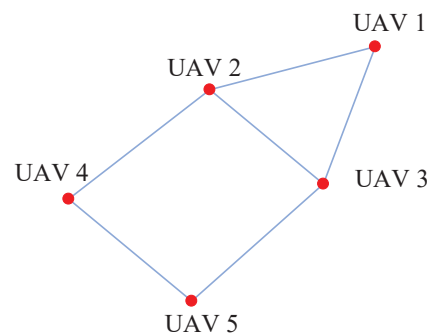


**Figure 2.** The communication topology.

The motion model of the target is described using a discrete-time state-space system [13]

$$\mathbf{x}_{k+1} = \begin{bmatrix} 1 & \frac{\sin \Omega_k T}{\Omega_k} & 0 & -\left(\frac{1-\cos \Omega_k T}{\Omega_k}\right) & 0 & 0 & 0 \\ 0 & \cos \Omega_k T & 0 & -\sin \Omega_k T & 0 & 0 & 0 \\ 0 & \frac{1-\cos \Omega_k T}{\Omega_k} & 1 & \frac{\sin \Omega_k T}{\Omega_k} & 0 & 0 & 0 \\ 0 & \sin \Omega_k T & 0 & \cos \Omega_k T & 0 & 0 & 0 \\ 0 & 0 & 0 & 0 & 1 & T & 0 \\ 0 & 0 & 0 & 0 & 0 & 1 & 0 \\ 0 & 0 & 0 & 0 & 0 & 0 & 1 \end{bmatrix} \mathbf{x}_k + \mathbf{w}_k$$

where  $\mathbf{x}_k = [x_k, \dot{x}_k, y_k, \dot{y}_k, z_k, \dot{z}_k, \Omega_k]^T$  is the state of the target;  $x_k, y_k,$  and  $z_k$  denote positions;  $\dot{x}_k, \dot{y}_k,$  and  $\dot{z}_k$  denote velocities in the  $x, y,$  and  $z$  directions, respectively; and  $\Omega_k$  is the unknown turn rate and  $T = 0.2$  s is the sampling time. The process noise  $\mathbf{w}_k$  is a zero-mean Gaussian with a covariance matrix  $\mathbf{Q} = \text{diag}\{q_1\mathbf{\Gamma}, q_1\mathbf{\Gamma}, q_1\mathbf{\Gamma}, q_2T\}$ , where

$$\mathbf{\Gamma} = \begin{bmatrix} T^3/3 & T^2/2 \\ T^2/2 & T \end{bmatrix}$$

and  $q_1 = 0.1 \text{ m/s}^3$  and  $q_2 = 1.75 \times 10^{-4} \text{ rad/s}^2$  denote the process noise intensity.

The UAVs are equipped with AOA sensors, whose measurement equation is [51]

$$z_k^i = \gamma_k^i \begin{bmatrix} \theta_k^i \\ \varphi_k^i \end{bmatrix} + \boldsymbol{\eta}_{i,k} = \gamma_k^i \left[ \begin{array}{c} \tan^{-1} \left( \frac{y_k - s_{iy}(k)}{x_k - s_{ix}(k)} \right) \\ \tan^{-1} \left( \frac{z_k - s_{iz}(k)}{\sqrt{(x_k - s_{ix}(k))^2 + (y_k - s_{iy}(k))^2}} \right) \end{array} \right] + \boldsymbol{\eta}_{i,k}$$

where  $\theta_k^i \in (-\pi, \pi]$  and  $\varphi_k^i \in [-\frac{\pi}{2}, \frac{\pi}{2}]$  are the true azimuth and elevation angles from the UAV  $i$  at time  $k$ , respectively;  $\tan^{-1}(\cdot)$  is the four-quadrant inverse tangent function. The measurement noise is  $\mathbf{R}_k^i = 0.05^2 \mathbf{I} \text{ rad}^2$ .

To evaluate the tracking performance, the root-mean square error (RMSE) of the position and velocity of the target estimated using the  $i$ th UAV at time  $k$  are, respectively, defined as [20]

$$\text{RMSE}_{k,\text{pos}}^i = \sqrt{\frac{1}{N_c} \sum_{j=1}^{N_c} \left[ (x_k^j - \hat{x}_{k,f}^{i,j})^2 + (y_k^j - \hat{y}_{k,f}^{i,j})^2 + (z_k^j - \hat{z}_{k,f}^{i,j})^2 \right]}$$

$$\text{RMSE}_{k,\text{vel}}^i = \sqrt{\frac{1}{N_c} \sum_{j=1}^{N_c} \left[ (\dot{x}_k^j - \hat{\dot{x}}_{k,f}^{i,j})^2 + (\dot{y}_k^j - \hat{\dot{y}}_{k,f}^{i,j})^2 + (\dot{z}_k^j - \hat{\dot{z}}_{k,f}^{i,j})^2 \right]}$$

where  $N_c$  is the total times of Monte Carlo runs;  $[x_k^j, y_k^j, z_k^j]^T$  and  $[\dot{x}_k^j, \dot{y}_k^j, \dot{z}_k^j]^T$  are the real position and velocity of the target at the  $j$ -th Monte Carlo run, respectively; and  $[\hat{x}_{k,f}^{i,j}, \hat{y}_{k,f}^{i,j}, \hat{z}_{k,f}^{i,j}]^T$  and  $[\hat{\dot{x}}_{k,f}^{i,j}, \hat{\dot{y}}_{k,f}^{i,j}, \hat{\dot{z}}_{k,f}^{i,j}]^T$  are the fusion estimate of the position and velocity estimated by the  $i$ th UAV, respectively.

To evaluate the consistency of the estimates, the disagreement of the estimates is defined as [6]

$$\rho_k = \sqrt{\sum_{i=1}^n \|\bar{\hat{\mathbf{x}}}_{k,f} - \hat{\mathbf{x}}_{k,f}^i\|^2}$$

where  $\bar{\hat{\mathbf{x}}}_{k,f} = \frac{1}{n} \sum_{j=1}^n \hat{\mathbf{x}}_{k,f}^j$  represents the mean of the estimate of all UAVs. If  $\rho_k$  increases, the deviation between the estimates of the UAVs also increase and this indicates a worse consistency for the estimates.

Furthermore, the average accumulative RMSEs (AARMSE) of the position and velocity of the whole target tracking system are adopted to assess the effectiveness of the proposed distributed path optimization method, which are respectively defined as [16]

$$\text{AARMSE}_{\text{pos}} = \sqrt{\frac{1}{n} \frac{1}{K} \sum_{i=1}^n \sum_{k=1}^K \left[ \left( x_k^i - \hat{x}_{k,f}^i \right)^2 + \left( y_k^i - \hat{y}_{k,f}^i \right)^2 + \left( z_k^i - \hat{z}_{k,f}^i \right)^2 \right]}$$

$$\text{AARMSE}_{\text{vel}} = \sqrt{\frac{1}{n} \frac{1}{K} \sum_{i=1}^n \sum_{k=1}^K \left[ \left( \dot{x}_k^i - \hat{\dot{x}}_{k,f}^i \right)^2 + \left( \dot{y}_k^i - \hat{\dot{y}}_{k,f}^i \right)^2 + \left( \dot{z}_k^i - \hat{\dot{z}}_{k,f}^i \right)^2 \right]}$$

The true initial state of the target is  $x_0 = [0 \text{ m}, 20 \text{ m/s}, 0 \text{ m}, 20 \text{ m/s}, 0 \text{ m}, 0 \text{ m/s}, -0.05 \text{ rad/s}]^T$ , and  $P_{0,f}^i = \text{diag}\{1000 \text{ m}^2, 100 \text{ m}^2/\text{s}^2, 1000 \text{ m}^2, 100 \text{ m}^2/\text{s}^2, 1000 \text{ m}^2, 100 \text{ m}^2/\text{s}^2, 10^{-4} \text{ rad}^2/\text{s}^2\}$ . The initial state estimate  $x_{0,f}^i$  of UAV  $i$  is chosen randomly from  $\mathcal{N}(x_0, P_{0,f}^i)$  in each Monte Carlo run. The initial positions of the UAVs are deployed randomly in the area of  $2000 \text{ m} \times 2000 \text{ m}$  at the height of  $800 \text{ m}$ . The detection probability is  $\lambda_i = 0.8$ . The velocity of the UAVs is  $50 \text{ m/s}$ . We set  $\delta = 1 \text{ m}$  for numerical approximation of gradients and  $N_c = 200$  for the Monte Carlo experiments.

The proposed method was compared with stationary platforms and the methods proposed in [38,39]. The positions of the stationary platforms were deployed as the initial positions of the UAVs. The DCKFI-CI was applied for target tracking with stationary platforms. In addition, the methods in [38,39] for distributed estimation and path optimization algorithms were adopted for comparison.

Figure 3 shows the trajectory of the target and the UAVs at the 200th Monte Carlo run. The UAVs continuously approached the target to achieve an improved tracking accuracy. This is due to the fact that the accuracy of tracking increases as an AOA sensor gets closer to the target [22]. Additionally, in the top view depicted in Figure 3b, we can observe that the UAVs also adjusted their angles with respect to each other and the target to enhance the tracking accuracy. Figure 4 shows the compared  $\text{RMSE}_{\text{pos}}$  and  $\text{RMSE}_{\text{vel}}$  of all UAVs. Figure 5 shows the compared  $\text{RMSE}_{\text{pos}}$  and  $\text{RMSE}_{\text{vel}}$  of UAV 1. As expected, the tracking performance was improved with the proposed method compared to the stationary platforms, the method in [38], and the method in [39].

Figure 6 shows the disagreement  $\rho_k$  of the estimates with the DCKFI-CI using the UAVs steered with the proposed path optimization method and stationary platforms. The disagreement  $\rho_k$  remained stable when  $\lambda_i$  was decreased from 0.8 to 0.5 for the proposed method and stationary platforms, which demonstrates that the estimation through DCKFI-CI exhibited good consistency. Additionally, it was also observed that the estimates using the UAVs exhibited better consistency compared to those with the static platform. This is attributed to the compression of error covariance through the acquisition of measurements via distributed path optimization, followed by the diffusion process that reduced the disagreement of the estimates.

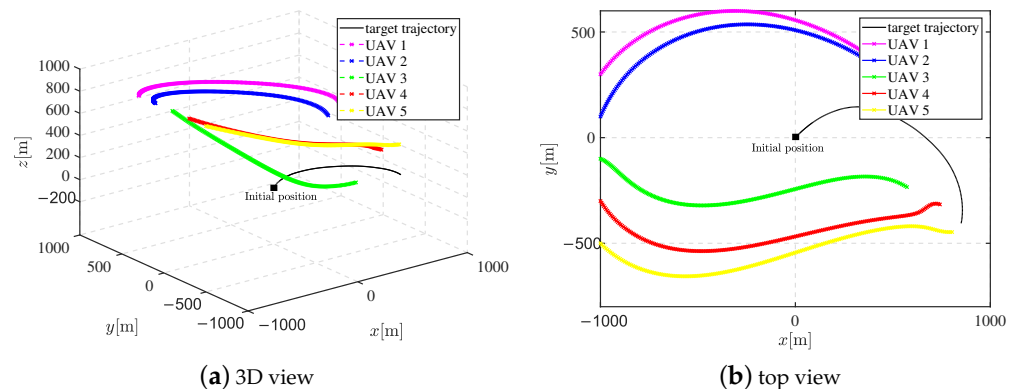
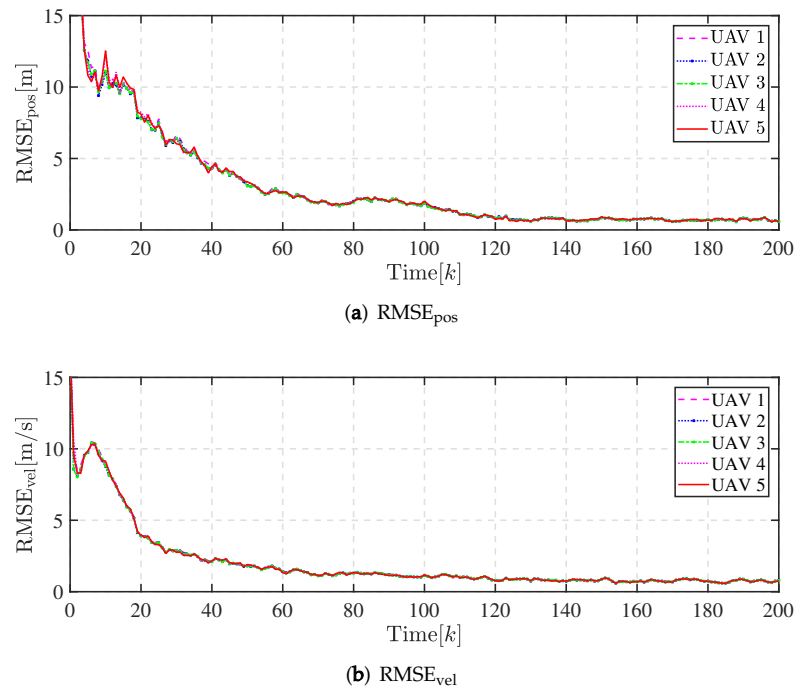
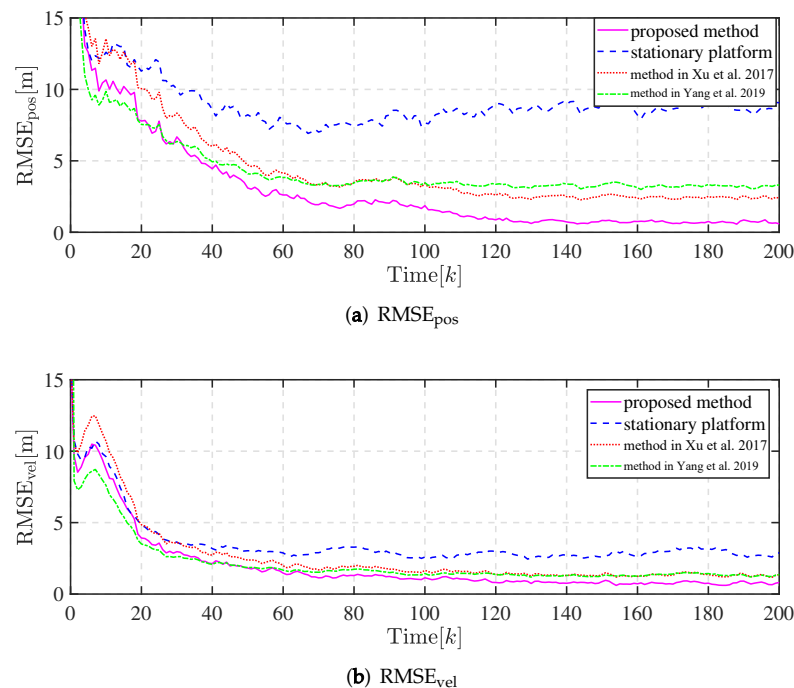


Figure 3. The trajectory of the UAVs for target tracking.



**Figure 4.** The tracking performance for all UAVs.

Furthermore, we compared the AARMSE under different detection probabilities of  $\lambda_i = 0.5$  and  $\lambda_i = 0.8$ . As shown in Table 1, the  $AARMSE_{pos}$  with the proposed method decreased 55.4%, 28.7%, and 28.1% compared with the stationary platforms, the method in [38], and the method in [39] when  $\lambda_i = 0.8$ . Meanwhile, the  $AARMSE_{vel}$  decreased 56.8%, 31.1%, and 29.3% when  $\lambda_i = 0.8$ . Similarly, the decrease in the  $AARMSE_{pos}$  when  $\lambda_i = 0.5$  was 53.8%, 30.1%, and 30.3% compared with the stationary platforms, the method in [38], and the method in [39]. The decrease in the  $AARMSE_{vel}$  was 48.5%, 23.4% and 21.6% compared with the mentioned methods. According to the above results, the proposed path optimization method significantly improved the tracking performance for the whole network with different detection probabilities.



**Figure 5.** Comparison of the tracking performance for UAV 1 [38,39].

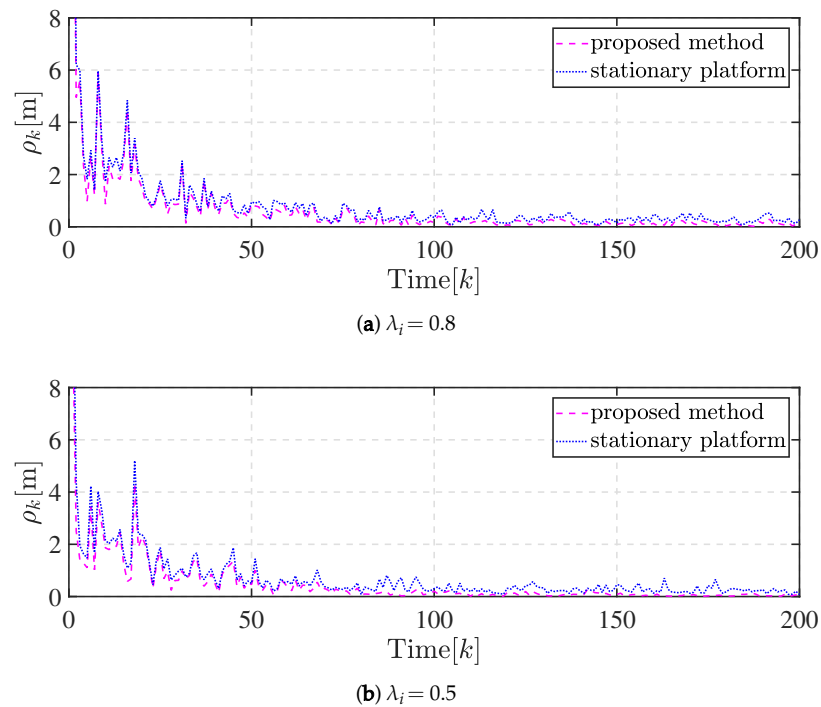


**Figure 6.** Comparison of the disagreement of the fusion estimates.

**Table 1.** Comparison of  $AARMSE_{pos}$  and  $AARMSE_{vel}$ .

	$\lambda_i$	$AARMSE_{pos}$ [m]	$AARMSE_{vel}$ [m/s]
Proposed method	0.5	4.38	2.79
	0.8	3.72	1.88
Stationary platforms	0.5	9.48	5.42
	0.8	8.35	4.36
Method in [38]	0.5	6.27	3.64
	0.8	5.22	2.73
Method in [39]	0.5	6.28	3.56
	0.8	5.17	2.66

## 7. Conclusions

In this paper, the problem of distributed state estimation with intermittent measurements for UAV target tracking was studied. Moreover, in order to further improve target tracking performance, distributed path optimization was considered. First, a diffusion cubature Kalman filter with intermittent measurements based on covariance intersection was proposed. Furthermore, an alternative transformation of DCKFI-CI based on the information form was developed by utilizing a pseudo measurement matrix. The performance of the proposed algorithm was analyzed with respect to the consistency of the estimate and the bound of the error covariance. With the DKFICI-CI algorithm, the estimates of the UAVs were robust against detection failure and exhibited good consistency for target tracking. In addition, a distributed UAV path optimization algorithm was developed to improve the tracking performance, by minimizing the sum of the traces of fused error covariance matrices based on exchanging the local estimate of the optimal solution with the cost function. The proposed method provided an enhancement of the whole tracking system. The simulations verified the effectiveness of the proposed method. The enhancement of the tracking performance was contingent on the exchange of information among the neighbour UAVs, which presents communication burdens. Meanwhile, the large amount of data poses a challenge to the limited computation power carried by UAVs. In order to alleviate these communication and computational burdens, we will incorporate event-triggered mechanisms [52,53] into data transmission and information processing in future works.

**Author Contributions:** Conceptualization, S.W.; methodology, S.W.; software, S.W.; validation, S.W. and Y.L.; formal analysis, S.W. and Y.L.; investigation, S.W. and Y.L.; resources, Y.L.; data curation, S.W.; writing—original draft preparation, S.W.; writing—review and editing, S.W., Y.L. and G.Q.; supervision, Y.L.; funding acquisition, Y.L. and A.S. All authors have read and agreed to the published version of the manuscript.

**Funding:** This work was supported in part by the National Natural Science Foundation of China (62171223 and 61871221).

**Institutional Review Board Statement:** Not applicable.

**Informed Consent Statement:** Not applicable.

**Data Availability Statement:** Not applicable.

**Conflicts of Interest:** The authors declare no conflict of interest.

## Nomenclature

$\gamma$	binary stochastic variable
$\hat{x}$	estimate of $x$
$f(\cdot)$	process function
$h(\cdot)$	measurement function
$k$	discrete time
$\eta$	measurement noise
$P$	estimate error covariance
$s$	UAV position
$w$	process noise
$x$	state vector
$z$	measurement vector
CI	covariance intersection
CRLB	Cramer–Rao lower bound
DCKFI	diffusion cubature Kalman filter with intermittent measurements
FIM	Fisher information matrix
UAV	unmanned aerial vehicle

## References

1. Javaid, S.; Saeed, N.; Qadir, Z.; Fahim, H.; He, B.; Song, H.; Bilal, M. Communication and Control in Collaborative UAVs: Recent Advances and Future Trends. *IEEE Trans. Intell. Transp. Syst.* **2023**, *24*, 5719–5739. [\[CrossRef\]](#)
2. Jeong, S.; Simeone, O.; Kang, J. Mobile Edge Computing via a UAV-Mounted Cloudlet: Optimization of Bit Allocation and Path Planning. *IEEE Trans. Veh. Technol.* **2018**, *67*, 2049–2063. [\[CrossRef\]](#)
3. Izzat, A.D.; Morched, D.; Housseem, J.; Fazal, Q.K.; Sadeeq, J.; Dimitris, P.; Tsaramirsis, G. A Technical Framework for Selection of Autonomous UAV Navigation Technologies and Sensors. *Comput. Mater. Contin.* **2021**, *68*, 2771–2790.
4. Alshammari, O.; Mahyuddin, M.N.; Jerbi, H. A Neural Network-Based Adaptive Backstepping Control Law With Covariance Resetting for Asymptotic Output Tracking of a CSTR Plant. *IEEE Access* **2020**, *8*, 29755–29766. [\[CrossRef\]](#)
5. Shi, L.; Li, W.; Shi, M.; Shi, K.; Cheng, Y. Opinion Polarization Over Signed Social Networks with Quasi Structural Balance. *IEEE Trans. Autom. Control* **2023**, 1–8. [\[CrossRef\]](#)
6. Olfati-Saber, R. Distributed Kalman filtering for sensor networks. In Proceedings of the 2007 46th IEEE Conference on Decision and Control, New Orleans, LA, USA, 12–14 December 2007; pp. 5492–5498. [\[CrossRef\]](#)
7. Olfati-Saber, R. Kalman-Consensus Filter : Optimality, stability, and performance. In Proceedings of the 48th IEEE Conference on Decision and Control (CDC) Held Jointly with 2009 28th Chinese Control Conference, Shanghai, China, 15–18 December 2009; pp. 7036–7042. [\[CrossRef\]](#)
8. Battistelli, G.; Chisci, L. Kullback–Leibler average, consensus on probability densities, and distributed state estimation with guaranteed stability. *Automatica* **2014**, *50*, 707–718. [\[CrossRef\]](#)
9. Cattivelli, F.S.; Sayed, A.H. Diffusion Strategies for Distributed Kalman Filtering and Smoothing. *IEEE Trans. Autom. Control* **2010**, *55*, 2069–2084. [\[CrossRef\]](#)
10. Hu, J.; Xie, L.; Zhang, C. Diffusion Kalman Filtering Based on Covariance Intersection. *IEEE Trans. Signal Process.* **2012**, *60*, 891–902. [\[CrossRef\]](#)
11. Li, W.; Jia, Y.; Du, J.; Meng, D. Diffusion Kalman filter for distributed estimation with intermittent observations. In Proceedings of the 2015 American Control Conference (ACC), Chicago, IL, USA, 1–3 July 2015; pp. 4455–4460. [\[CrossRef\]](#)

12. Julier, S.; Uhlmann, J.; Durrant-Whyte, H. A new method for the nonlinear transformation of means and covariances in filters and estimators. *IEEE Trans. Autom. Control* **2000**, *45*, 477–482. [[CrossRef](#)]
13. Arasaratnam, I.; Haykin, S. Cubature Kalman Filters. *IEEE Trans. Autom. Control* **2009**, *54*, 1254–1269. [[CrossRef](#)]
14. Cattivelli, F.S.; Sayed, A.H. Distributed nonlinear Kalman filtering with applications to wireless localization. In Proceedings of the 2010 IEEE International Conference on Acoustics, Speech and Signal Processing, Dallas, TX, USA, 14–19 March 2010; pp. 3522–3525. [[CrossRef](#)]
15. Battistelli, G.; Chisci, L. Stability of Consensus Extended Kalman Filtering for Distributed State Estimation. *IFAC Proc. Vol.* **2014**, *47*, 5520–5525. [[CrossRef](#)]
16. Li, W.; Wei, G.; Han, F.; Liu, Y. Weighted Average Consensus-Based Unscented Kalman Filtering. *IEEE Trans. Cybern.* **2016**, *46*, 558–567. [[CrossRef](#)]
17. Lefebvre, T.; Bruyninckx, H.; De Schuller, J. Comment on “A new method for the nonlinear transformation of means and covariances in filters and estimators” [with authors’ reply]. *IEEE Trans. Autom. Control* **2002**, *47*, 1406–1409. [[CrossRef](#)]
18. Chen, H.; Wang, J.; Wang, C.; Shan, J.; Xin, M. Distributed diffusion unscented Kalman filtering based on covariance intersection with intermittent measurements. *Automatica* **2021**, *132*, 109769. [[CrossRef](#)]
19. Wang, G.; Li, N.; Zhang, Y. Diffusion nonlinear Kalman filter with intermittent observations. *Proc. Inst. Mech. Eng. Part G J. Aerosp. Eng.* **2018**, *232*, 2775–2783. [[CrossRef](#)]
20. Bar-Shalom, Y.; Li, X.R.; Kirubarajan, T. *Estimation with Applications to Tracking and Navigation: Theory Algorithms and Software*; John Wiley & Sons: New York, NY, USA, 2004.
21. Ucinski, D. *Optimal Measurement Methods for Distributed Parameter System Identification*; CRC Press: Boca Raton, FL, USA, 2004.
22. Bishop, A.N.; Fidan, B.; Anderson, B.D.; Doğançay, K.; Pathirana, P.N. Optimality analysis of sensor-target localization geometries. *Automatica* **2010**, *46*, 479–492. [[CrossRef](#)]
23. Zhao, S.; Chen, B.M.; Lee, T.H. Optimal sensor placement for target localisation and tracking in 2D and 3D. *Int. J. Control* **2013**, *86*, 1687–1704. [[CrossRef](#)]
24. Fang, X.; Yan, W.; Zhang, F.; Li, J. Optimal Sensor Placement for Range-Based Dynamic Random Localization. *IEEE Geosci. Remote Sens. Lett.* **2015**, *12*, 2393–2397. [[CrossRef](#)]
25. Xu, S.; Doğançay, K. Optimal Sensor Placement for 3-D Angle-of-Arrival Target Localization. *IEEE Trans. Aerosp. Electron. Syst.* **2017**, *53*, 1196–1211. [[CrossRef](#)]
26. Xu, S.; Ou, Y.; Wu, X. Optimal sensor placement for 3-D Time-of-Arrival Target Localization. *IEEE Trans. Signal Process.* **2019**, *67*, 5018–5031. [[CrossRef](#)]
27. Li, Y.; Qi, G.; Sheng, A. Optimal deployment of vehicles with circular formation for bearings-only multi-target localization. *Automatica* **2019**, *105*, 347–355. [[CrossRef](#)]
28. Martínez, S.; Bullo, F. Optimal sensor placement and motion coordination for target tracking. *Automatica* **2006**, *42*, 661–668. [[CrossRef](#)]
29. Hung, N.T.; Crasta, N.; Moreno-Salinas, D.; Pascoal, A.M.; Johansen, T.A. Range-based target localization and pursuit with autonomous vehicles: An approach using posterior CRLB and model predictive control. *Robot. Auton. Syst.* **2020**, *132*, 103608. [[CrossRef](#)]
30. Oshman, Y.; Davidson, P. Optimization of observer trajectories for bearings-only target localization. *IEEE Trans. Aerosp. Electron. Syst.* **1999**, *35*, 892–902. [[CrossRef](#)]
31. Chung, T.H.; Burdick, J.W.; Murray, R.M. A decentralized motion coordination strategy for dynamic target tracking. In Proceedings of the 2006 IEEE International Conference on Robotics and Automation, Orlando, FL, USA, 15–19 May 2006; IEEE: Piscataway, NJ, USA, 2006; pp. 2416–2422.
32. Doganay, K. Online Optimization of Receiver Trajectories for Scan-Based Emitter Localization. *IEEE Trans. Aerosp. Electron. Syst.* **2007**, *43*, 1117–1125. [[CrossRef](#)]
33. Tharmarasa, R.; Kirubarajan, T.; Lang, T. Joint path planning and sensor subset selection for multistatic sensor networks. In Proceedings of the 2009 IEEE Symposium on Computational Intelligence for Security and Defense Applications, Ottawa, ON, Canada, 8–10 July 2009; pp. 1–8. [[CrossRef](#)]
34. Zhou, K.; Roumeliotis, S.I. Optimal motion strategies for range-only constrained multisensor target tracking. *IEEE Trans. Robot.* **2008**, *24*, 1168–1185. [[CrossRef](#)]
35. Meng, W.; Xie, L.; Xiao, W. Communication aware optimal sensor motion coordination for source localization. *IEEE Trans. Instrum. Meas.* **2016**, *65*, 2505–2514. [[CrossRef](#)]
36. Abichandani, P.; Lobo, D.; Muralidharan, M.; Runk, N.; McIntyre, W.; Bucci, D.; Benson, H. Distributed Motion Planning for Multiple Quadrotors in Presence of Wind Gusts. *Drones* **2023**, *7*, 58. [[CrossRef](#)]
37. Doğançay, K. Single-and multi-platform constrained sensor path optimization for angle-of-arrival target tracking. In Proceedings of the 2010 18th European Signal Processing Conference, Aalborg, Denmark, 23–27 August 2010; IEEE: Piscataway, NJ, USA, 2010; pp. 835–839.
38. Xu, S.; Doğançay, K.; Hmam, H. Distributed pseudolinear estimation and UAV path optimization for 3D AOA target tracking. *Signal Process.* **2017**, *133*, 64–78. [[CrossRef](#)]
39. Yang, Z.; Zhu, S.; Chen, C.; Guan, X.; Feng, G. Distributed path optimisation of mobile sensor networks for AOA target localisation. *IET Control Theory Appl.* **2019**, *13*, 2817–2827. [[CrossRef](#)]

40. Doğançay, K. UAV Path Planning for Passive Emitter Localization. *IEEE Trans. Aerosp. Electron. Syst.* **2012**, *48*, 1150–1166. [[CrossRef](#)]
41. He, S.; Shin, H.S.; Tsourdos, A. Trajectory Optimization for Target Localization With Bearing-Only Measurement. *IEEE Trans. Robot.* **2019**, *35*, 653–668. [[CrossRef](#)]
42. Dai, J.; Pu, W.; Yan, J.; Shi, Q.; Liu, H. Multi-UAV Collaborative Trajectory Optimization for Asynchronous 3-D Passive Multitarget Tracking. *IEEE Trans. Geosci. Remote Sens.* **2023**, *61*, 5101116. [[CrossRef](#)]
43. Nedic, A.; Ozdaglar, A. Distributed Subgradient Methods for Multi-Agent Optimization. *IEEE Trans. Autom. Control* **2009**, *54*, 48–61. [[CrossRef](#)]
44. Nedić, A.; Olshevsky, A.; Shi, W. Achieving Geometric Convergence for Distributed Optimization Over Time-Varying Graphs. *SIAM J. Optim.* **2017**, *27*, 2597–2633. [[CrossRef](#)]
45. Qu, G.; Li, N. Harnessing Smoothness to Accelerate Distributed Optimization. *IEEE Trans. Control. Netw. Syst.* **2018**, *5*, 1245–1260. [[CrossRef](#)]
46. Li, W.; Qin, K.; Li, G.; Shi, M.; Zhang, X. Robust bipartite tracking consensus of multi-agent systems via neural network combined with extended high-gain observer. *ISA Trans.* **2023**, *136*, 31–45. [[CrossRef](#)] [[PubMed](#)]
47. Kluge, S.; Reif, K.; Brokate, M. Stochastic Stability of the Extended Kalman Filter With Intermittent Observations. *IEEE Trans. Autom. Control* **2010**, *55*, 514–518. [[CrossRef](#)]
48. Julier, S.; Uhlmann, J. A non-divergent estimation algorithm in the presence of unknown correlations. In Proceedings of the 1997 American Control Conference (Cat. No.97CH36041), Albuquerque, NM, USA, 6 June 1997; Volume 4, pp. 2369–2373. [[CrossRef](#)]
49. Almasri, M.M.; Alajlan, A.M.; Elleithy, K.M. Trajectory Planning and Collision Avoidance Algorithm for Mobile Robotics System. *IEEE Sens. J.* **2016**, *16*, 5021–5028. [[CrossRef](#)]
50. Pang, Z.H.; Zheng, C.B.; Sun, J.; Han, Q.L.; Liu, G.P. Distance- and Velocity-Based Collision Avoidance for Time-Varying Formation Control of Second-Order Multi-Agent Systems. *IEEE Trans. Circuits Syst. II Express Briefs* **2021**, *68*, 1253–1257. [[CrossRef](#)]
51. Farina, A. Target tracking with bearings – only measurements. *Signal Process.* **1999**, *78*, 61–78. [[CrossRef](#)]
52. Tabuada, P. Event-Triggered Real-Time Scheduling of Stabilizing Control Tasks. *IEEE Trans. Autom. Control* **2007**, *52*, 1680–1685. [[CrossRef](#)]
53. Liang, Y.; Li, Y.; Chen, Y.; Sheng, A. Event-triggered diffusion nonlinear estimation for sensor networks with unknown cross-correlations. *Syst. Control Lett.* **2023**, *175*, 105506. [[CrossRef](#)]

**Disclaimer/Publisher’s Note:** The statements, opinions and data contained in all publications are solely those of the individual author(s) and contributor(s) and not of MDPI and/or the editor(s). MDPI and/or the editor(s) disclaim responsibility for any injury to people or property resulting from any ideas, methods, instructions or products referred to in the content.